JOURNAL OF APPLIED ELECTROCHEMISTRY 9 (1979) 233–242

Inhibition and nickel electrocrystallization

J. AMBLARD, I. EPELBOIN, M. FROMENT, G. MAURIN

Physique des Liquides et Electrochimie, Groupe de Recherche no. 4 du CNRS associé à l'Université Pierre et Marie Curie, 4 Place Jussieu, 75230 Cedex 05, France

Received 27 June 1978

The electrocrystallization of Ni is known to be a highly inhibited process. This work gives some conclusions about the nature of the major inhibiting species. All of these species are formed in the catholyte because of the hydrogen codeposition. Depending on plating conditions, mainly pH and current density of metallic deposition, we observe a predominancy of a definite inhibitor which selectively promotes one mode of growth and leads to a deposit exhibiting definite structural properties. A careful structural investigation of Ni deposits obtained from a Watts solution, thanks to both X-ray diffractometry and electron-microscope techniques, leads us to distinguish a free mode of growth, which is characterized by [100] oriented deposits, from several inhibited modes such as ⟨110⟩, [210], ⟨211⟩ and ⟨111⟩. The two latter are stabilized by $Ni(OH)_2$ while the two former are respectively due to atomic and molecular forms of adsorbed hydrogen.

1. Introduction

Inhibition, a basic concept extensively studied by Professor H. Fischer [1–3], must be expected to play a major role in the electrocrystallization of metals from their aqueous solutions, both because of the existence of a solvent and of the great complexity of the phenomena involved in that kind of deposition process. This seems to be especially true for a transition metal like nickel, which has been described as electrochemically inert [4], since its high surface energy is responsible for its great ability to adsorb any kind of chemical species which may exist close to a Ni^{2+}–Ni interface. However, there are many such chemisorbable species (like H^+, OH^-, metallic adions, anions, additives, etc.) and a relevant problem is to find out which among them exerts the predominant effect in given electrolysis conditions.

The great merit of Professor H. Fischer's pioneering work is the emphasis he put on the correlation between inhibition and its effect on morphological features of electrodeposits, as revealed by micrographs taken very often from their cross-sections. This led him to distinguish five types of deposits (see [1] p. 424) according to the way their crystallites are arranged on the cathodic substrate. But techniques of structural investigation have now been considerably improved, so that further progress can be made, both in the description of the various crystallites a deposit is made of and in the description of their preferred orientations. The first aim of our paper is to present and discuss the results of a careful structural analysis of Ni electrodeposits obtained from a Watts solution in various plating conditions. All these deposits belong to the FT class (field-oriented texture type) according to Fischer's nomenclature [3].

Maybe the most important structural feature of such deposits is their *texture*, i.e. the non-random orientation distribution of their crystallites. A quite amazing fact is that the texture of thick deposits (several μm or 10 μm, depending on plating conditions [5]) is completely independent of the substrate orientation and appears to be only governed by electrochemical parameters: we have shown that, for a given electrolyte composition, texture mainly depends on cathodic potential (or current density if the temperature is kept constant) and pH of the solution [6]. This observation suggests that, following Fischer's example, this effect of electrochemical parameters may eventually be discussed in terms of inhibition: an evident source of inhibition is the formation of hydroxide (or more generally basic salts) close to the Ni^{2+}–Ni

interface when the solution pH is too high. Such species severely hinder Ni crystal growth, so that a coherent deposit cannot be obtained for media of $pH_{sol} > 5$. Another source is the abundant hydrogen evolution in very acid media. One can then imagine that there is a medium pH domain where both types of inhibition play a minor role. The same kind of considerations may be developed regarding the effect of current density: in the low current density range the metallic surface is much more sensitive to any strong adsorbants since there is practically no renewal due to the crystallization process; a dynamic release is to be expected for higher current densities because of a greater growth rate; but for the highest current densities there again appears a new source of inhibition, which comes from the slowness of the dehydration process as compared to the metallic ions incorporation. Then the risk of deposits incorporating some decomposition products arises. Here again we can suppose a domain of medium current densities where inhibition is at a minimum. Of course such considerations remain essentially qualitative and they have to be more closely related to the experimentally observed structural features of Ni deposits. Further, a second aim of our paper is to propose an interpretation for the origin of texture during Ni electrocrystallization. This interpretation points out the close correlation existing between the stability of a definite texture under given electrolysis conditions and the predominancy inside the cathodic layer of a definite chemical inhibiting species.

2. Experimental

We knew from experience that the structural properties of Ni electrodeposits strongly depend on plating conditions. Thus special care has been taken to control every electrolysis parameter. Details are given elsewhere [7]. The solution is a typical Watts bath, composed of $NiSO_4 . 7H_2O$ ($300\,g\,l^{-1}$) $NiCl_2 . 6H_2O$ ($35\,g\,l^{-1}$) and boric acid ($40\,g\,l^{-1}$). Its pH is adjusted to the working value with slight additions of either concentrated H_2SO_4 or NH_4OH. Organic additives are very often used to modify certain physical properties of Ni deposits (their brightness for example) and they markedly affect textures. We have chosen to examine the behaviour of two compounds, butyne diol and sodium benzene sulphonate, which are quite well representative of the two classes of standard addition agents: levelling agents or/and brighteners. For that purpose the solution is maintained at a constant pH_{sol} value (4·5) and we progressively add small amounts of organic compounds, up to $50 \times 10^{-3}\,mol\,l^{-1}$. The temperature is 50° C in all cases and stirring is ensured by rotation of the cathode at a constant angular velocity ($2000\,rev\,min^{-1}$). The substrate is the front face of a mechanically-polished brass cylinder.

Once the deposits are thick enough (we need at least 50 μm [8]), they are rinsed with distilled water, dried and then submitted to several techniques of structural investigation. Their fibre-like texture is first studied by X-ray diffractometry, thanks to a method giving a complete, quantitative texture analysis [8, 9]. We determine not only the Miller indices $[hkl]$ but also the dispersion σ_{hkl}, the perfection Q_{hkl} and the volume ratio t_{hkl} of crystallites for each texture component. Then we submit the deposits to different electron-microscopy techniques, which provide information about their surface morphology [5, 10] or about the internal organization of their crystallites [11–13]. The conjugated use of both methods shows that Ni deposits exhibiting different textures grow by completely different mechanisms [14]. Hence the determination of a texture axis is not a mere indication of a greater tendency for the deposit fibres to possess a definite crystallographic direction along the electric-field direction. It means chiefly that the fibres have a quite specific internal organization and, moreover, that they result from a definite growth mechanism.

3. Results

We shall present below first the results for deposits obtained from an organic-free Watts solution operated at different pH and current densities, then the texture modifications provoked by addition of either butynediol or benzene sulphonate to the basic solution maintained at $pH_{sol} = 4·5$.

3.1. *Deposits from an organic-free bath*

As mentioned before, the pH range for our study is limited towards alkaline values at $pH_{sol} = 5$.

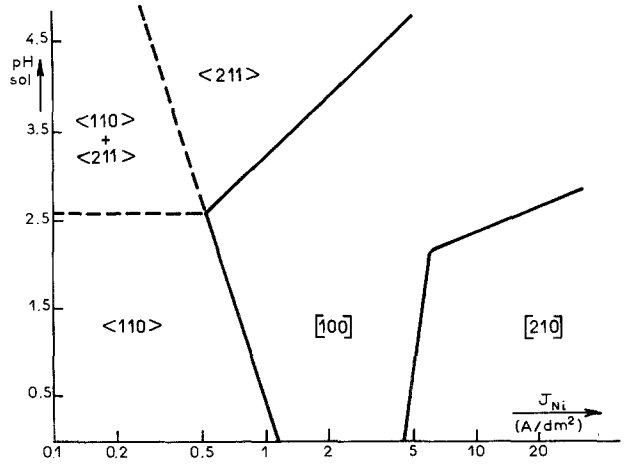

Fig. 1. Stability of the various fibre textures of nickel electrodeposits versus pH of the Watts' bath and nickel current density.

Beyond that limit Ni deposits are no longer coherent, due to the inhibiting effect of $Ni(OH)_2$. The other relevant parameter, cathodic potential, is somewhat difficult to calculate because of a large ohmic drop correction [7]. Thus we would rather plot our results against the Ni partial current density J_{Ni}, which is directly proportional to the growth rate of the metallic layer. The value of J_{Ni} is computed from thickness measurements at the points of the disc cathode where the deposit is thinnest. A diagram gives the correspondence between J_{Ni} values and the measured densities of the electrolysis current [7, 9].

Fig. 1 gives the stability diagram for the various textures encountered in Ni electrodeposits when pH_{sol} is varied from 0–5 and J_{Ni} over more than two decades, which corresponds to growth rates from 0·3–100 nm per second for the Ni layer. This diagram is made up of five domains, four among them corresponding to one-component textures. The last domain, for high pH_{sol} values and low current densities, corresponds to deposits exhibiting both ⟨1 1 0⟩ and ⟨2 1 1⟩ preferred orientations, with a predominancy (greater perfection) of ⟨110⟩. All these deposits are made of a compact array of fibres, the lengths of which depend on the fibre axis: ⟨1 1 0⟩ and [2 1 0] exhibit the shortest fibres, while fibres of ⟨2 1 1⟩ and [1 0 0] orientations are better developed [7, 9]. The quantitative analysis of the textural perfection as a function of pH_{sol} shows a degradation of [1 0 0] deposits and conversely an improvement of [2 1 0] when going to more acid media. Such a behaviour suggests that [2 1 0] is favoured (and [1 0 0] hindered) by the strong hydrogen evolution occurring in very acid media for highly cathodic potentials.

This hypothesis [9] has been recently confirmed by a complementary study of [2 1 0] perfection as a function of bath temperature and stirring efficiency [15], which proves that the best [2 1 0] textures are encountered in conditions (low temperature, low stirring) favouring an inhibition of Ni growth by gaseous hydrogen. A first set of experiments, the results of which are given in Table 1, illustrates the effect of bath temperature, from 45–30° C, when keeping constant the current density ($J_{Ni} \sim 4\ A\ dm^{-2}$). This table shows that, all other parameters being kept constant, a decrease of temperature leads to the replacement of [1 0 0] by [2 1 0]. Moreover, the lower the bath temperature, the more perfect (= less dispersed) is the [2 1 0] texture and the poorer becomes the current efficiency.

A second set of experiments concerns the study of the effect on the same texture of the stirring efficiency, which is varied by changing the velocity Ω of our rotating disc cathode from 150–4000 rev min^{-1},

Table 1. Effect of bath temperature on quantitative parameters of [2 1 0] texture and current efficiency.

Bath temperature (° C)	*Texture axis*	*Dispersion* σ_{210}	*Perfection* Q_{210}	*Current efficiency* (%)
45	[1 0 0]	–	–	83
40	[2 1 0]	7·7°	34	78
35	[2 1 0]	5·5°	48	71
30	[2 1 0]	4·8°	78	66

Table 2. Influence of stirring efficiency on the dispersion of [210] texture

σ_{210}	Ω (rev min^{-1})
10·6°	4000
9·2°	3000
8·6°	2000
8·2°	1500
7·8°	1000
5·3°	500
4·6°	150

for given values of bath temperature (40° C) and current density (3 A dm^{-2}). The results are reported in Table 2. They show a clear tendency towards less-dispersed textures for lower values of stirring efficiency.

Both sets of experiments support the hypothesis of a close relationship between the stability of [210] and a strong inhibition of the growing Ni interface by hydrogen evolution.

These textural features have to be completed by electron-microscope data showing the crystallites internal structure for each texture. Such data [10–14] reveal a deep difference between ⟨110⟩ and ⟨211⟩ on the one hand and [100] and [210] on the other. While the latter do not show any structural peculiarities, the former have a quite specific internal organization where crystallites systematically contain a given number of vertical twin planes which give them either a twofold or a fivefold symmetry. Fig. 2 is a transmission micrograph of a thin foil from a ⟨211⟩ deposit, which shows that crystallites exhibiting such an orientation are divided into two parts by groups of twins of uneven number [10]. Fig. 3 corresponds to a ⟨110⟩ deposit containing crystallites with fivefold symmetries; electron-micro-diffraction proves that such crystallites are made up of five identical parts separated by {111} twin planes and possessing a common ⟨110⟩ axis. Hence crystallites of both ⟨211⟩ and ⟨110⟩ are never single crystals. On the basis of some work on silver electrocrystallization we have now strong evidence that such peculiar organizations find their origin in the formation of three-dimensional atomic clusters exhibiting perfect icosahedral or decahedral struc-

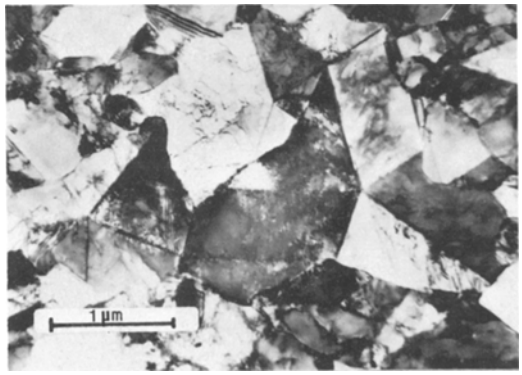

Fig. 3. Transmission electron micrograph of a nickel electrodeposit exhibiting a ⟨110⟩ preferred orientation. Notice the five convergent twin planes in most of the grains.

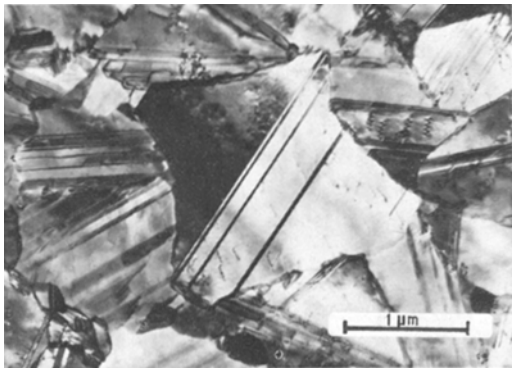

Fig. 2. Transmission electron micrograph of a nickel electrodeposit exhibiting a ⟨211⟩ preferred orientation. Notice the parallel twin planes crossing the grains.

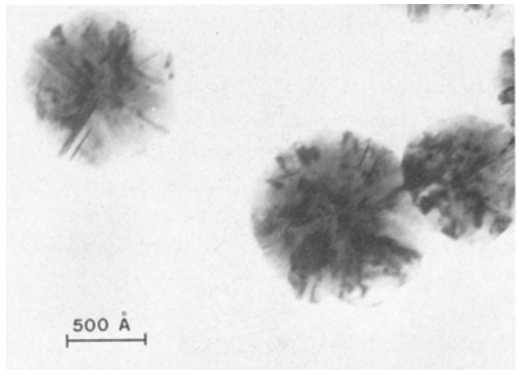

Fig. 4. Multitwinned icosahedral microcrystallites included in a (100) epitaxial single crystal nickel electrodeposit, observed with a 1 MeV transmission electron microscope by Thevenin [28].

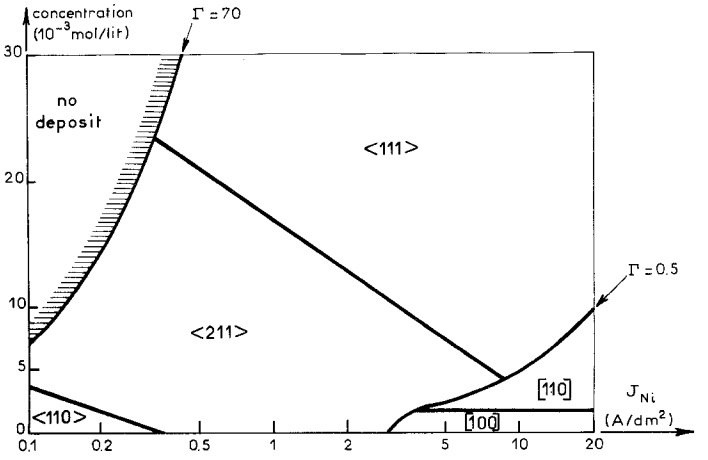

Fig. 5. Stability of various fibre textures of nickel electrodeposits versus nickel current density and concentration of butyne-2-diol 1,4 as inhibitor.

tures [16] and that this new type of nucleation has to be related to a strong inhibition of the electrocrystallization process. These anomalous structures appear even during epitaxial growth of nickel deposited on various faces of a single crystal. They have been directly observed by using high voltage transmission electron microscopy (Fig. 4) [28]. Because of the great consequences they have for the deposits properties (for instance the sharp growth anisotropy induced by the presence of twin planes [12–14]), we shall distinguish by the symbol ⟨ ⟩ the textures formed throughout this mode of nucleation from all others denoted by the symbol [ ].

3.2. *Bright deposits*

Both butynediol and sodium benzene sulphonate exert an effect of grain refinement, thus producing brighter deposits with textures of lesser perfection, but they modify the texture axes in a quite specific way, which is illustrated by the diagrams of respectively Figs. 5 and 6.

3.2.1. *Effect of butynediol.* The texture diagram of Fig. 5 summarizes the modifications provoked by an addition of increasing amounts of butynediol (but-2-yne 1,4 diol) into the Watts solution, up to concentrations of 30×10^{-3} mol l^{-1}. Starting from the reference state, which is the ⟨1 1 0⟩ → ⟨2 1 1⟩ → [1 0 0] texture axes sequence for increasing current densities in an organic-free bath, we move to a quick disappearance of both ⟨1 1 0⟩ and [1 0 0] textures, connected with a remarkable stability of the ⟨2 1 1⟩ orientation. We must note the presence of a small domain, for medium concentrations and high current densities, where a [1 1 0] orientation appears (noted as $[1\,1\,0]^{B}$ in our previous papers [11–14]) which is entirely different from the above described ⟨1 1 0⟩ texture (previously noted as $[1\,1\,0]^{A}$). The main discrepancy originates in the way crystallites of both textures are formed. Only ⟨1 1 0⟩ crystallites degenerate from non-crystalline atomic aggregates with icosahedral or decahedral structures, while crystallites of [1 1 0] texture are formed according to another nucleation process.

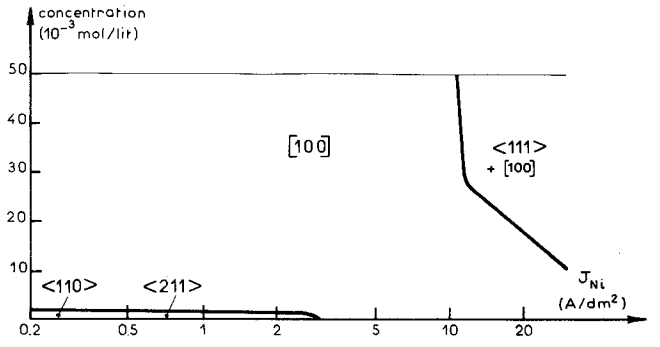

Fig. 6. Stability of various fibre textures of nickel electrodeposits versus nickel current density and concentration of sodium benzene sulphonate as inhibitor.

The ⟨2 1 1⟩ texture itself is replaced by a ⟨1 1 1⟩ texture for the highest additive concentrations. We have shown that the appearance of such a new texture occurs when the main cathodic reaction is no more the metallic deposition but the hydrogen discharge, greatly enhanced by the catalytic saturation of the —C≡C— bond onto the nickel surface [7]. Crystallites of that ⟨1 1 1⟩ orientation are very small and then not easily observable by electron-microscopy techniques. We have shown by X-ray diffraction that they contain numerous twins and are roughly spherical in shape. Thus they are very likely icosahedra formed according to the same nucleation process as ⟨1 1 0⟩ and ⟨2 1 1⟩ crystallites.

The levelling properties of butynediol involve a very rapid adsorption and consumption of the acetylenic alcohol on the Ni cathode. Thus we think that its bulk concentration C is not a relevant parameter for describing the disturbance it brings during Ni electrocrystallization: it seems better to consider the ratio $\Gamma = C/J_{Ni}$, which also takes into account the kinetic effect of the permanent renewal of the metallic surface. Such a parameter, introduced [7, 17] as the *dynamic concentration* of the additive, governs not only the transition of textures like [1 0 0] and [1 1 0] towards inhibited modes of growth like ⟨2 1 1⟩ and ⟨1 1 1⟩, but even the limit beyond which no coherent deposit can be obtained (see the diagram of Fig. 5). Moreover, it even governs the textures' perfection in every domain of the same diagram [7]. It must be noted that, while any texture except ⟨1 1 1⟩ is disturbed by butynediol (Q_{hkl} diminishes as Γ increases), an opposite dependence may be observed for ⟨1 1 1⟩: Q_{111} increases with Γ. It proves that this highly disturbed ⟨1 1 1⟩ mode of growth is the unique mode being actually favoured by the presence of the unsaturated diol. The appearance of ⟨1 1 1⟩ only occurs when all other modes of growth are severely inhibited.

However, because of both the brightening properties of butynediol and the remark made above about its levelling power, it is not possible to consider the diol itself as the main source of inhibition. Thus we have been led to suppose that this inhibition more likely stems from the abundant formation of $Ni(OH)_2$ near the cathode, due to the important pH rise provoked there by the diol-enhanced hydrogen consumption [17].

3.2.2. *Effect of benzene sulphonate.* When using this other type of brightener, we must first of all note a great difference of behaviour from the preceding case. This difference not only resides in the way benzene sulphonate affects Ni textures, but also in the manner in which it intervenes in the cathodic hydrogen codeposition.

The texture diagram of Fig. 6 shows that, beyond a concentration of 2×10^{-3} mol l^{-1}, ⟨1 1 0⟩ and ⟨2 1 1⟩ textures disappear in favour of [1 0 0], which is stable almost everywhere, except in a marginal domain (of both highest current densities and concentrations), where a predominant ⟨1 1 1⟩ component appears. Thus it was possible to make a quantitative analysis of the [1 0 0] texture perfection in the whole domain [7]. Results show that, provided the additive dynamic concentration is great enough ($\Gamma \geqslant 10^{-3}$ mol A^{-1} dm^{-1}) to ensure an important coverage of the cathode surface, Q_{100} depends no more, either on C or on Γ. It then only depends on J_{Ni}, that is to say on the crystal growth rate, according to the law

$$Q_{100} \propto J_{Ni}^{-1/2}.$$

Thus, contrary to the case of butynediol, the disturbance occurring in Ni electrocrystallization due to the presence of benzene sulphonate does not depend on its dynamic concentration. Such a behaviour must be related to other kinetic results taken from the literature. We know that the inhibiting effect of this aromatic compound is not transport-controlled, as was the case for butynediol [18]. Thus the sulphonate compound probably undergoes a very slow cathodic process after its adsorption: this process has been described as a hydrogenolysis of the C–S bond [19, 20] followed by a desorption of the aromatic ring and sulphur incorporation [21, 22] along the ⟨1 1 0⟩ directions [23].

It is of interest to note that such a very long process influences the discharge competition between Ni^{2+} and H^+ ions: sites occupied by the cumbersome benzene ring are no longer vacant for H^+ discharge and adsorption. That, in a certain way, benzene sulphonate hinders particularly hydrogen codeposition may also be concluded from the study of pH_{sol} variations during Ni deposition. We have measured a permanent increase of pH_{sol} during the deposition of Ni from organic-free solutions; this increase is highly

enhanced (sometimes by a factor 10^2) by butynediol. Conversely, the addition of benzene sulphonate is accompanied by no variation of pH_{sol}. An exception has to be made here for the domain where ⟨1 1 1⟩ appears; then a variation becomes noticeable, which may be related to a hydrogenation of the benzene ring [7]. Another indication that sulphonates exert a hindering effect for the hydrogen codeposition is the observation of their reducing effect on the internal stresses of Ni deposits [21, 24]. At last, it seems quite surprising that such long-staying molecules, partially incorporated in Ni deposits, do not provoke (as butynediol did) an increase of the number of dislocations [25] within the deposits!

4. Discussion

We shall first present our interpretation of texture formation in Ni electrodeposits, then examine its implications in the concept that one may have about the mechanism of Ni electrocrystallization both from crystallographic and kinetic standpoints.

4.1. *Mechanism of texture formation*

Two main kinds of theoretical explanation had been proposed earlier to account for the appearance of a texture in Ni electrodeposits. It is not our purpose to discuss them in great detail (see [26]). But let us only recall the major points.

The first hypothesis assumes that texture results from a competitive nucleation [27]; different two-dimensional nuclei are first formed, the orientation of which only depends on cathodic overvoltage. But such an assumption is inconsistent with recent experimental data [28] which prove that, even under a strong epitaxial influence, the same variety of three-dimensional nuclei are formed onto a Ni surface, whatever the current density (Fig. 4). Hence, as we observe only one kind of crystallite in the steady state mode of growth, texture must result more from a *growth competition* between the various kinds of nuclei. The parameters governing such a competition now have to be elucidated.

The second hypothesis [29] starts with the correct idea of a growth competition, more or less governed by the surface coverage of atomic adsorbed hydrogen (H_{ads}). However, two main objections can be raised to that kind of standpoint: the theory only considers a competition occurring between single crystals, and we have seen that crystallites of either ⟨1 1 0⟩, ⟨2 1 1⟩ or ⟨1 1 1⟩ textures are necessarily polycrystalline; moreover, H_{ads} is far from being the sole chemical species capable of inhibiting the growth process.

Thus, we have to consider a growth competition between nuclei of different kinds, with which several kinds of inhibiting species interfere. We have already shown in Section 3.1 that the [2 1 0] orientation must be related to a strong inhibition of Ni electrocrystallization by H_2 evolution. Let us see if other orientations may be specifically related to other chemical inhibiting species.

First of all, in what plating conditions may we expect the strongest inhibition by H_{ads}? Starting from the equilibrium potential for the Ni^{2+}/Ni system, we know that Ni deposition begins as soon as the H^+ discharge becomes diffusion-controlled [30], for a cathodic overvoltage of about 190 mV in our conditions. Thus, in the low current density range, the metallic surface must be almost entirely covered with H_{ads}, which has been experimentally confirmed [31]. It is no longer the case for higher current densities because of a release of the cathodic surface (thanks to its renewal) without newly arriving H^+ becoming discharged and adsorbed. Then we must note that the ⟨1 1 0⟩ preferred orientation is stable in the very domain where we may expect the strongest inhibition by H_{ads}. This result has been recently confirmed in our laboratory by electrochemical impedance measurements carried out by Bressan and Wiart [46]. These authors showed that impedance diagrams obtained at low current densities and corresponding to ⟨1 1 0⟩ texture formation have an inductive loop which can be attributed to hydrogen adsorption. When intensity increases, this loop and the ⟨1 1 0⟩ texture disappear at the same time (Wiart, Discussion of [26]).

The fact that H^+ ions arriving at a Ni cathode are readily discharged and adsorbed leads to an impoverishment of protons in the cathodic layer, and then a marked pH rise of the catholyte [32, 33], which may cause a precipitation of $Ni(OH)_2$ close to the Ni/catholyte interface. Examination of the Pourbaix diagram for Ni [34] shows under

which conditions the strongest inhibition by $Ni(OH)_2$ must be expected: both for low current densities and less-acid media, that would correspond to the conditions where we find ⟨2 1 1⟩ oriented deposits. Now the problem is: does an actual coincidence exist between the domain of stability for $Ni(OH)_2$ in the Pourbaix diagram and the domain of stability of ⟨2 1 1⟩ in our texture diagram of Fig. 1? Of course not, because the former is related to thermodynamic equilibria, while the latter only refers to kinetic results. The comparison between both diagrams [26] shows that both domains are shifted the one versus the other, both in pH (the difference is 3·6 pH units) and in potential scales (the difference is about 260 mV). But we may ascribe both differences to the kinetic effect of hydrogen codeposition, which simultaneously inhibits the Ni surface and raises the local pH value. Under that assumption, we consider that $Ni(OH)_2$ is responsible for the stability of ⟨2 1 1⟩ in Ni electrodeposits.

Lastly, what can be said about the [1 0 0] orientation? We have seen that this texture is hindered by H_2 evolution. From the above considerations about ⟨2 1 1⟩, it is clear that [1 0 0] disappears when there is a predominancy of $Ni(OH)_2$ in the catholyte. And the same orientation is also hindered by H_{ads}, since it appears only when the metallic surface is dynamically released from that adsorbant. Therefore, we consider this orientation as corresponding to the *free mode of growth* for electrolytic Ni. This hypothesis is consistent with data taken from the literature, which show that [1 0 0]-oriented Ni deposits exhibit the highest ductility [35] and the lowest internal stress and hardness [36]. And we know further that it is on a (1 0 0)-oriented Ni substrate that epitaxial growth gives the best results [37, 38].

Of course, we must be cautious about that notion of 'freedom' for the [1 0 0] mode of growth: it does not mean that the growing surface is entirely free from any adsorbant (such as (NiOH), for example, a very often quoted intermediate species in Ni electrocrystallization mechanisms [39, 40]); it only means that the metallic surface is less hindered by every species directly related to the hydrogen codeposition. Conversely, it may be covered by species, like $(NiOH)_{ads}$, which play a relevant role in the metallic deposition.

4.2. *Implications*

So it seems possible to ascribe specifically every observed texture in a Ni electrodeposit to a definite inhibiting species. May we go as far as to say that the species ($Ni(OH)_2$ for example) 'favours' a given mode of growth (⟨2 1 1⟩ in our example)? A careful examination of our data allows us to conclude that it is better to adopt just the opposite standpoint: $Ni(OH)_2$ inhibits Ni deposition very strongly, that is why no coherent deposit can be obtained for $pH_{sol} > 5$. The ⟨2 1 1⟩ mode of growth is less inhibited than the others, though it is inhibited too. We made an analysis of Q_{211} as a function of pH which proves that a pH increase is accompanied by a reduction of the ⟨2 1 1⟩ textural perfection [7, 9]. And our results about butynediol show the same tendency: even the ⟨2 1 1⟩ mode of growth disappears when too much acetylenic alcohol is added to the solution, that is to say when too much $Ni(OH)_2$ is formed in the catholyte.

All these facts suggest that we must discuss Ni electrogrowth essentially in kinetic terms. There is a permanent growth competition of several kinds of nuclei, each of them growing according to a specific mode. The growth competition is governed by the dynamic composition of the cathodic layer. This composition depends both on the local pH value and on the electrochemical balance of the various cathodic reactions occurring at a given imposed potential (which means mainly the different reactions of the competitive discharge of Ni^{2+} and H^+ ions). The chemical species which are then formed are adsorbed, more or less strongly, on the different available sites, in such a way that they may block growth sites, slow down propagation steps or modify the activity of emerging structural defects, etc. They behave quite specifically according both to their chemical nature and to the crystallographic arrangement of their adsorption sites. We already know, for example, that different single crystal faces of Ni present huge differences of behaviour towards epitaxial growth [37, 38, 41–44]. This probably originates from the way they adsorb various inhibitors like H_{ads}, $Ni(OH)_2$, (NiOH), H_2O, etc. But we shall have to find out and describe more precisely what are the crystallographic reasons for the observed differential

sensitivity of various modes of Ni growth to various inhibitors.

The same kinetic point of view allows us to explain the consequences of a change in the plating conditions for the deposit properties, among others its texture. Regarding the effect of organic additives, for example, their activity during Ni deposition has sometimes been ascribed to their preferential adsorption on various Ni reticular planes [14, 44]. But we now know, from the results given in Section 3.2, that we must first of all examine how they react on the cathode and what role they play in the Ni^{2+}/H^{+} competition: a slow-reacting brightener such as benzene sulphonate disturbs the high-rate Ni deposition more, while a quick-reacting leveller like butynediol disturbs mainly the low-rate deposits. The former hinders more hydrogen codeposition than Ni^{2+} reduction; it then favours the formation of [1 0 0] deposits with low internal stress. The latter enhances more hydrogen discharge; it then provokes the abundant formation of $Ni(OH)_2$ which stabilizes ⟨2 1 1⟩ and ⟨1 1 1⟩ textures in highly stressed deposits.

Lastly, we have to examine what are the consequences of our hypothesis for the Ni electrocrystallization mechanism. The first mechanism we proposed [40], on the basis of an electrochemical impedance analysis [18], concerned Ni deposits obtained from a Watts solution operated at a pH_{sol} of 4·5 and medium current densities. It outlined the fundamental role in these conditions of the adsorbed intermediate $(NiOH)_{ads}$. But other mechanisms may eventually intervene in other plating conditions: in acid media, for example, another mechanism was advanced as an alternative [45], where adsorbed forms of hydrogen play a major role. And we now believe, according to the present results, that several other galvanic paths must be imagined to describe the transition from a Ni solvated cation to an incorporated Ni metallic atom, each of them involving some degree of interference with the hydrogen codeposition. As a matter of fact, some recent impedance measurements during Ni deposition from a Watts bath at $pH_{sol} = 1{\cdot}5$ clearly show, besides the relaxation of $(NiOH)_{ads}$, the relaxation of two other species, which are likely to be two different kinds of adsorbed hydrogen [46].

Implying simultaneously several galvanic paths, the whole mechanism of Ni electrocrystallization is probably very complex. However, we may suppose that, in given plating conditions, one of these paths is predominant, doubtless the one in which the same inhibiting species responsible for the texture observed in these conditions intervenes.

5. Conclusions

This work shows the outstanding importance of inhibition in the case of Ni electrocrystallization. Starting from a whole set of structural data collected through X-ray diffraction analysis and electron-microscope investigations of thick deposits, it has been possible to ascribe a definite inhibitor to each observed texture. [1 0 0], which may be associated with the adsorbed intermediate $(NiOH)_{ads}$, is regarded as the free mode of growth for electrolytic Ni. The three other textures, encountered in deposits from an organic-free solution, are associated with the predominancy inside the cathodic layer of a chemical species which results from hydrogen codeposition: H_{ads} stabilizes ⟨1 1 0⟩, gaseous H_2 favours [2 1 0] and $Ni(OH)_2$ inhibits every mode of growth except ⟨2 1 1⟩. In conditions of more severe inhibition, that is to say when an organic additive consumes much more cathodic hydrogen, ⟨2 1 1⟩ is replaced by ⟨1 1 1⟩.

Thus we have been led to point out the major role of cathodic hydrogen codeposition and all its consequences upon the cathodic layer composition. On this composition depend, not only the kind of predominant inhibitor but also the structural properties of the deposit and maybe the actual mechanism of Ni electrocrystallization also.

References

[1] H. Fischer, 'Elektrolytische Abscheidung und Elektrokristallisation von Metallen', Springer, Berlin (1954).
[2] *Idem*, *Electrodep. Surf. Treat.* **1** (1973) 239.
[3] *Idem*, *ibid* **1** (1973) 319.
[4] R. Piontelli and G. Serravalle, *Trans. Inst. Metal Finishing* **34** (1957) 293.
[5] M. Froment and A. Ostrowiecki, *Métaux Corrosion Ind.* **487** (1966) 83.
[6] M. Froment, G. Maurin and J. Thevenin, *Comptes Rendus Acad. Sci. Paris* **264C** (1967) 1520.
[7] J. Amblard, thesis, Paris (1976).
[8] J. Amblard, M. Froment and G. Maurin, *Electrodep. Surf. Treat.* **2** (1974) 205.

[9] J. Amblard, M. Froment and N. Spyrellis, *Surf. Technol.* **5** (1977) 205.
[10] G. Maurin and M. Froment, *Métaux Corrosion Ind.* **487** (1966) 103.
[11] M. Froment and G. Maurin, *J. Microscopie* 7 (1968) 39.
[12] G. Maurin, *Oberfläche-Surface* **11** (1970) 297 309.
[13] *Idem, ibid* **12** (1971) 8, 24, 47, 54.
[14] I. Epelboin, M. Froment and G. Maurin, *Plating* **56** (1969) 1356.
[15] J. Amblard, M. Froment and S. Vitkova, Communication at the *28th ISE Meeting* Druzhba near Varna (1977) p. 427.
[16] I. Epelboin, M. Froment and G. Maurin, *ibid* p. 371.
[17] J. Amblard, Th. Costavaras, A. Hugot-Le Goff and N. Spyrellis, *Oberfläche-Surface* **18** (1977) 1.
[18] R. Wiart, *ibid* 9 (1968) 213, 241, 273.
[19] H. Brown, *Plating* **55** (1968) 1047.
[20] I. Dubsky and P. Kozak, *Metalloberfläche* **24** (1970) 423.
[21] R. J. Kendrick, *Trans. Inst. Met. Finishing* **40** (1963) 19.
[22] H. Brown, Comm. at *Interfinish* Bâle (1972) p. 114.
[23] M. Froment, G. Maurin and J. Thevenin, *J. Microscopie* 8 (1969) 521.
[24] A. Knödler, *Metalloberfläche* **20** (1966) 52.
[25] M. Froment, *J. Microscopie* **3** (1964) 61.
[26] J. Amblard and M. Froment, Communication at the *12th Faraday Symposium* Southampton (1977) p. 136.
[27] N. A. Pangarov, *J. Electroanalyt. Chem.* 9 (1965) 70.
[28] J. Thevenin, *J. Microsc. Spectr. Electron* 1 (1976) 7.
[29] A. K. N. Reddy and S. R. Ragagopalan, *J. Electroanalyt. Chem.* 6 (1963) 141, 153, 159.
[30] R. K. Dorsch, *ibid* **21** (1969) 495.
[31] I. Epelboin, P. Morel and H. Takenouti, *J. Electrochem. Soc.* **118** (1971) 1282.
[32] A. G. Ives, J. W. Edington and G. B. Rothwell, *Electrochim. Acta* **15** (1970) 1797.
[33] S. I. Berezina, L. V. Burnasheva, A. N. Gil'manov, I. Kh. Muzeev and R. M. Sageeva, *Elektrokhimiya* **10** (1974) 948.
[34] M. Pourbaix, MAtlas d'équilibres électrochimiques à 25° C', Gauthier Villars, Paris (1963) p. 333.
[35] F. Denise and H. Leidheiser Jr., *J. Electrochem. Soc.* **100** (1953) 490.
[36] D. J. Evans, *Trans. Faraday Soc.* **54** (1958) 1086.
[37] B. Rivolta, L. Peraldo Bicelli and G. Razzini, *J. Phys. D: Appl. Phys.* 8 (1975) 2025.
[38] M. Froment, G. Maurin and J. Thevenin, *Comptes Rendus Acad. Sci. Paris* **269C** (1969) 1367.
[39] J. Matulis and R. Slizys, *Electrochim. Acta* 9 (1964) 1177.
[40] I. Epelboin and R. Wiart, *J. Electrochem. Soc.* **118** (1971) 1577.
[41] H. Leidheiser Jr. and A. T. Gwathmey, *ibid* 98 (1951) 225.
[42] K. R. Lawless, *Phys. Thin Films* 4 (1967) 191.
[43] S. K. Verma and H. Wilman, *J. Phys. D: Appl. Phys.* 4 (1971) 1167.
[44] J. Thevenin, thesis, Paris (1974).
[45] B. Le Gorrec and J. Guitton, *Comptes Rendus Acad. Sci. Paris* **272C** (1971) 1784, 2031.
[46] J. Bressan, I. Epelboin, R. Wiart, Communication of the Department of Chemistry, Acad. Sci. Bulgaria, Special Issue in honour of Professor Kaischew (in press).